

Time-Dependent Quantum Dynamics Study of the Ne + H₂⁺ ($\nu = 0-9$) and D₂⁺ ($\nu = 0-12$) Proton Transfer Reactions at Thermal Collision Energies[†]

Jordi Mayneris-Perxachs and Miguel González*

Departament de Química Física i IQTC, Universitat de Barcelona, C/Martí i Franquès 1, 08028 Barcelona, Spain

Received: November 28, 2008; Revised Manuscript Received: January 5, 2009

The Ne + H₂⁺ and D₂⁺ proton transfer reactions were studied (reaction probabilities (P) and cross sections (σ)) using the time-dependent real wave packet quantum dynamics method at the centrifugal sudden level (CS-RWP method). This was made considering the influence of vibrational excitation of H₂⁺ and D₂⁺ on the dynamics ($(\nu = 0-9, j = 0)$ and $(\nu = 0-12, j = 0)$ vibrorotational states, respectively) at thermal collision energies ($E_{\text{col}} = 0.010$ to 0.14 eV). The CS-RWP relative cross sections at thermal collision energy (300 K) for Ne + H₂⁺ and Ne + D₂⁺ are in good agreement with the experimental data. The present results suggest the adequacy of the approach used here in describing these and related systems at thermal collision energies and from low to high vibrational excitation of reactants.

I. Introduction

Ion–molecule reactions can be relevant in many interesting situations, for example, interstellar processes, electric discharges, and planetary ionospheres. Although they can be explored at a wide range of collision energies (E_{col}) and are available to be studied in molecular beam experiments, there are often serious difficulties in performing theoretical studies because electronically nonadiabatic processes involving different potential energy surfaces (PESs) may easily occur as a result of the energetic proximity of the PESs.¹

The aim of the present work was to investigate the moderately endoergic proton transfer elementary reactions in the gas phase Ne + H₂⁺ ($\nu = 0-9, j = 0$) → NeH⁺ + H and Ne + D₂⁺ ($\nu = 0-12, j = 0$) → NeD⁺ + D under thermal collision energies ($\Delta D_0^\circ = 12.5$ kcal·mol⁻¹ for Ne + H₂⁺ → NeH⁺ + H) while paying attention to the influence of vibrational excitation and collision energy on reactivity and analyzing the intermolecular isotope effect.

Reactants and products adiabatically correlate on the ground PES, 1²A', of the NeH₂⁺ system, which has a collinear [Ne – H – H]⁺ minimum placed along the minimum energy path (MEP). This reaction differs from the more complex Ar + H₂⁺ and Kr + H₂⁺ reactions where several PESs are involved. This feature makes the Ne + H₂⁺ system very attractive for high-level theoretical studies, and it has been previously studied at low to moderate collision energies.²

The Ne + H₂⁺ reaction has been the subject of several experimental³⁻⁷ and theoretical studies.^{2,8-15} The last three experimental contributions were focused on investigating the influence of vibrational excitation of H₂⁺ and D₂⁺ on the reactivity, which was also the main objective of this work, and in refs 13 and 14, exact time-independent quantum dynamics calculations were performed on Ne + H₂⁺ ($\nu = 0-2, j = 0$). (See also ref 2.)

Here, to study the reactions Ne + H₂⁺ ($\nu = 0-9, j = 0$) and Ne + D₂⁺ ($\nu = 0-12, j = 0$), we applied the time-dependent

real wave packet (RWP) method¹⁶ using the centrifugal sudden (CS) approximation¹⁷ to determine the influence of vibrational excitation of reactants on reaction probabilities and reaction cross sections under thermal E_{col} values (0.010 to 0.14 eV). This complements a recent study carried out by our group on Ne + H₂⁺ ($\nu = 0-4, j = 0$) → NeH⁺ + H at moderate to intermediate collision energies (~ 0.3 to 1.7 eV)² where the CS-RWP method was also employed. To the best of our knowledge, this is the first high-level quantum dynamics calculation where the influence of very high vibrational levels of reactants on the dynamics has been investigated.

This Article is organized as follows. Section II briefly describes the computational method, and in Section III the results and discussion are given. The summary and conclusions are presented in Section IV.

II. Computational Methods

Because the theoretical approach used here coincides with that of ref 2, only a brief description will be given here. We calculated quantum reaction probabilities (P) via the RWP method of Gray and Balint-Kurti,¹⁶ defining an initial wave packet at a total angular momentum quantum number (J) in reactant Jacobi coordinates (R, r , and γ) and propagating only the real part of it on the best analytical ground PES of the NeH₂⁺ system available (PHHJ-3 surface)⁹ by using the CS approximation.¹⁷ The RWP method in the context of different approximations (CS and J -shifting methods) has been successfully applied to a variety of triatomic and tetraatomic reactions (see, e.g., refs 2 and 16–23).

The reaction probability at a fixed total angular momentum, $P^J(E_{\text{col}})$, is obtained for a range of E_{col} values from a single RWP propagation by using a flux method.²⁴ Despite the large initial distance employed, for large J values, the initial wave packet is not placed well enough in the asymptotic region, and to correct this fact, we used the backward propagation method.² From the corrected reaction probabilities, the reaction cross sections summed over all final quantum states (σ) are calculated from well-known expressions.²

The details of the initial wave packet, as well as the grid and other parameters employed in the CS-RWP calculations, are

[†] Part of the special issue "George C. Schatz Festschrift".

* Corresponding author. E-mail: miguel.gonzalez@ub.edu. Fax: +34-93-402 12 31.

TABLE 1: Parameters of the CS-RWP Calculations^a

parameters	Ne + H ₂ ^{+b}	Ne + D ₂ ⁺
scattering coordinate (<i>R</i>) range	0–31	0–37
number of grid points in <i>R</i>	258	308
grid spacing along <i>R</i>	0.12	0.12
internal coordinate (<i>r</i>) range	0.5–21	0.5–21
number of grid points in <i>r</i>	171	171
grid spacing along <i>r</i>	0.12	0.12
number of angular basis functions	50	50
potential and centrifugal cutoff	0.44	0.44
<i>R</i> and <i>r</i> absorption start at	25 and 15	31 and 15
<i>R</i> and <i>r</i> absorption strength	0.0005	0.0005
center of initial WP (<i>R</i> ₀)	24	30
width parameter of the WP ^c	0.39	0.28
initial relative translational energy/eV	0.02154	0.02154

^a All quantities are given in atomic units unless otherwise indicated. ^b These calculations were completed before the other calculations, using a smaller grid because the reaction conditions were less demanding than those considered in our previous work on Ne + H₂⁺. ^c These values were selected to reproduce the thermal collision energy distribution at 500 K, which has a most probable collision energy of 0.02154 eV.

listed in Table 1. Essentially, the same set of parameters as that obtained from our previous CS-RWP study on Ne + H₂⁺ ($v = 0-4$, $j = 0$)² was used here after some checks to ensure convergence for Ne + D₂⁺.

We calculated the reaction cross sections by employing *J* values in the range $0 \leq J \leq J_{\max}$, where the *J*_{max} value depends on the reaction and vibrational level (Table 2). To converge the propagation of the wave packet, 25 000 steps (iterations) were necessary, and this required about 10 h on a P-IV Xeon 2.8 GHz (2 GB of RAM) single processor.

III. Results and Discussion

A. Reaction Probabilities. The principal features of the CS-RWP reaction probabilities for the title reactions are very similar to those previously obtained in the study of Ne + H₂⁺ at moderate and intermediate collision energies.² Therefore, they exhibit a strong oscillatory behavior as a function of collision or total energy with the presence of sharp resonances (Figure 1). Because the analysis of resonances is rather demanding and far from the main purpose of this work, it will be only briefly mentioned here. These resonances and their effect on the reaction cross section were previously considered at an exact quantum dynamics level¹⁴ and also for $J = 0$.¹⁰ They appear because metastable states are important in the dynamics, and these states may arise from either a purely dynamical basis or a mixed contribution resulting from the influence of the [Ne–H–H]⁺ minimum of the PES and dynamical trapping due to effective potential barriers.

Figure 1 shows the reaction probability versus total energy for Ne + H₂⁺ ($v = 2, 4, 6$, and 8 , $j = 0$) → NeH⁺ + H at some *J* values. The threshold energy progressively moves to higher *E*_{total} values as *J* increases because the centrifugal barrier increases with *J*, as previously reported, and the increase in *J* also leads to a quenching of the resonances found in the reaction probabilities, as expected.²

B. Reaction Cross Sections. The CS-RWP reaction cross sections of Ne + H₂⁺ and Ne + D₂⁺ for several vibrational levels selected are shown in Figure 2. Because these reactions correspond to late barrier systems (where the barrier here corresponds to the reaction endoergicity), vibrational energy is more efficient than relative translational energy for the reaction to occur, as we have also seen in a previous study.² As vibrational excitation of the molecular ion increases, its efficiency progressively diminishes, and reactivity becomes rather insensitive to it at the higher vibrational levels examined, as expected. This behavior is more evident for Ne + D₂⁺.

For vibrational levels of reactants higher than $v = 3$, the reactions become exoergic with respect to the production of NeX⁺ ($v' = 0$, $j' = 0$) ($X = \text{H}$ and D), and because the PES is barrierless, the reaction cross section decreases with collision energy. The general shape of the σ versus *E*_{col} dependence is the typical one for reactions without threshold energy. Moreover, for all initial conditions (*E*_{col}, v , $j = 0$), the cross section for Ne + H₂⁺ is higher than that for Ne + D₂⁺. The same behavior has been observed in quasi-classical trajectory (QCT) calculations performed on these reactions.¹⁵ A somewhat deeper analysis of the intermolecular isotope effect will be presented in Section III.D.

Finally, it is interesting to point out that because of the sharp resonances exhibited by the reaction probabilities, after the partial wave sum carried out to determine the reaction cross sections, they are not completely quenched. Therefore, the dependence of the cross section with energy still shows the presence of oscillations. This behavior was also observed in a recent CS-RWP study on the Ne + H₂⁺ ($v = 0-4$, $j = 0$) reaction at moderate and intermediate collision energies² and also, for example, in previous time-independent exact quantum dynamics calculations^{13,14} carried out at lower energies than those of ref 2. It was for Ne + H₂⁺ ($v = 0-2$, $j = 0$) that for the first time in an accurate (CS) quantum calculation an oscillatory behavior was found in the σ versus *E*_{total} dependence.^{11,12}

C. Relative Reaction Cross Sections. There is no experimental information about the reaction cross section of reactions Ne + H₂⁺ (v) and Ne + D₂⁺ (v) under these conditions. However, from photoelectron-product ion delayed coincidence experiments, measurements of the relative reaction cross sections of Ne + H₂⁺ and D₂⁺ were reported^{5,25} for the same vibrational levels investigated here ($\sigma_{\text{rel}}(v) = \sigma(v)/\sum \sigma(v)$, where the sum extends over all vibrational levels investigated for each system) at thermal collision energy (300 K). In these experiments, the molecular ions were produced at a thermal rotational state distribution corresponding to room temperature. However, some classical trajectory calculations carried out by us on these systems showed that this amount of rotational excitation (with respect to $j = 0$) has little effect on reactivity. Hence, it makes sense to compare our CS-RWP σ_{rel} results for the molecular ions in (v , $j = 0$) with the experimental ones (v , j -distribution at room temperature). The theoretical and experimental data are shown in Figure 3. Of course, for Ne + H₂⁺ ($v = 0-1$) and Ne + D₂⁺ ($v = 0-2$), the experimental σ_{rel} values should be considered to be equal to zero because under the reactions

TABLE 2: *J* Intervals for Which CS-RWP Reaction Probabilities Were Calculated, as a Function of the Reaction and Vibrational Levels Selected

reaction/ <i>v</i>	0	1	2	3	4	5	6	7	8	9	10	11	12
Ne + H ₂ ⁺	0–20	0–20	0–32	0–44	0–46	0–46	0–48	0–48	0–54	0–56			
Ne + D ₂ ⁺	0–20	0–20	0–24	0–44	0–60	0–60	0–62	0–64	0–66	0–68	0–68	0–72	0–74

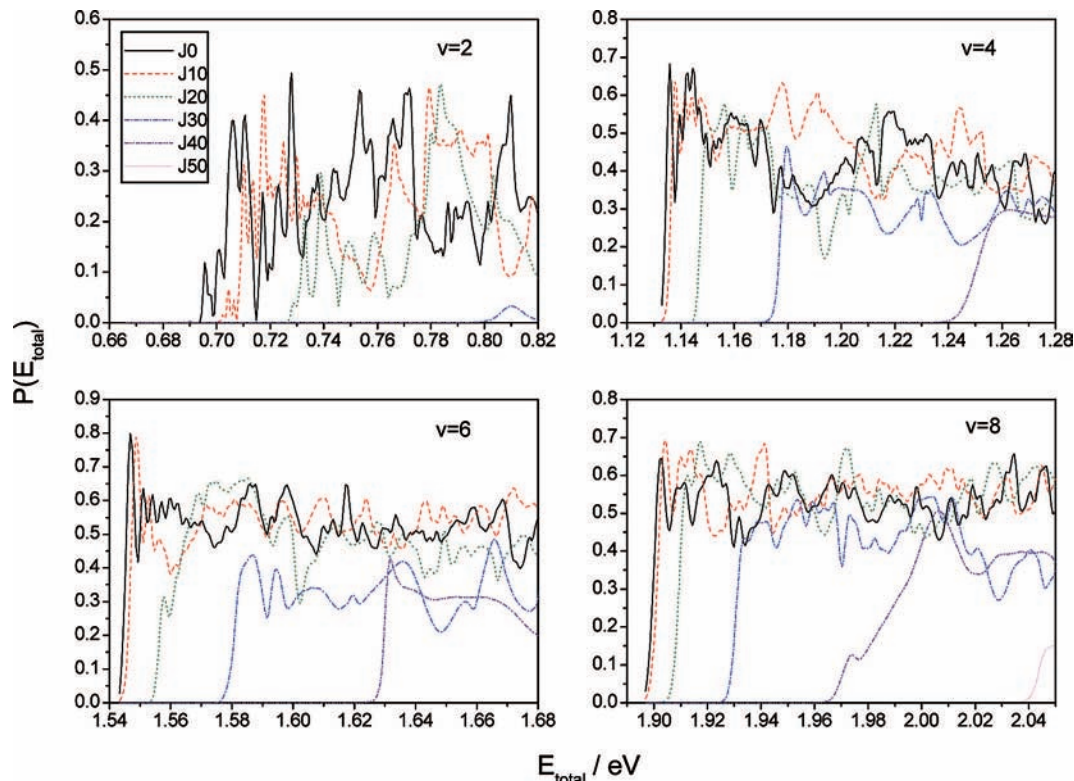


Figure 1. CS-RWP reaction probability of Ne + H₂⁺ ($v = 2, 4, 6,$ and $8, j = 0$) → NeH⁺ + H for selected J values as a function of total energy.

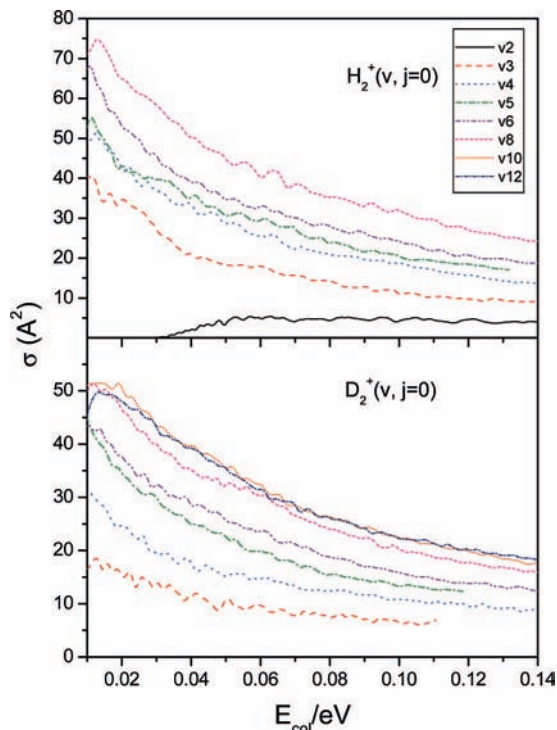


Figure 2. CS-RWP reaction cross sections of Ne + H₂⁺ ($v, j = 0$) and Ne + D₂⁺ ($v, j = 0$) for selected vibrational levels as a function of collision energy.

conditions examined, the production of NeH⁺ + H and NeD⁺ + D is energetically closed.

For Ne + H₂⁺ (v) under thermal collision energy conditions (E_{col} (300 K)), there is no reactivity up to $v = 2$, σ_{rel} increases significantly from $v = 2$ to 3, and the increase in σ_{rel} becomes smaller as v increases. The agreement with the measured

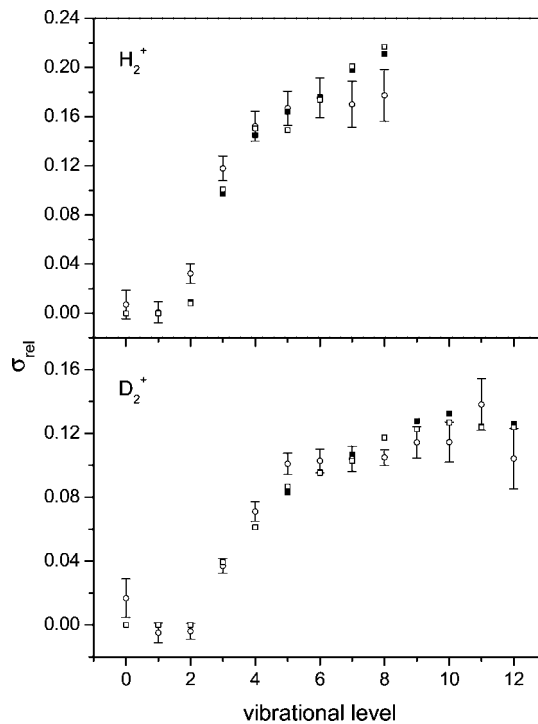


Figure 3. CS-RWP (\square and \blacksquare) and experimental (\circ)^{5,25} relative reaction cross sections of Ne + H₂⁺ ($v = 0-8, j = 0$) and Ne + D₂⁺ ($v = 0-12, j = 0$) as a function of the vibrational level. The symbols \square and \blacksquare correspond to the thermal E_{col} distribution at 300 K and to the average E_{col} value (0.0388 eV) at this temperature, respectively.

values⁵ is good, taking into account the experimental error bars. Moreover, quite similar results are obtained in the theoretical study when instead of the E_{col} distribution at 300 K, the average value of E_{col} at this temperature (0.0388 eV) is considered.

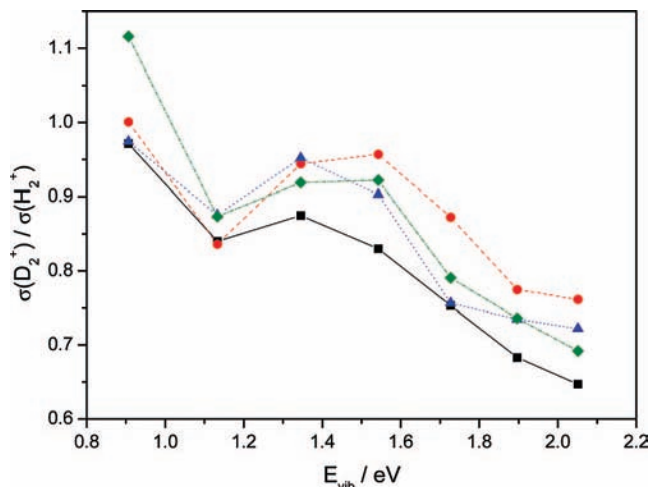


Figure 4. CS-RWP $\sigma(\text{Ne} + \text{D}_2^+)/\sigma(\text{Ne} + \text{H}_2^+)$ ratio as a function of the vibrational energy content of the molecular ion (E_{vib} , eV, $j = 0$) at selected E_{col} values: 0.015 (■), 0.040 (●), 0.080 (▲), and 0.120 (◆) eV. See the text.

The σ_{rel} of $\text{Ne} + \text{D}_2^+$ (ν) at E_{col} (300 K) exhibits a similar behavior to that found for $\text{Ne} + \text{H}_2^+$ (ν), although here reactivity is evident for only $\nu \geq 3$, and the initial increase in σ_{rel} with ν is not as strong as it is in the $\text{Ne} + \text{H}_2^+$ (ν) case, with a plateau being reached at around $\nu \geq 6$. Theoretical results also compare well with the experiment,⁵ and quite similar results are obtained when $E_{\text{col}} = 0.0388$ eV is used in the calculations.

D. Isotope Effect. To compare the reactivity of the systems as a function of vibrational excitation, four representative collision energies were selected. For comparison (same collisional, vibrational, and rotational energy for the two reactions), we selected the vibrational energies (E_{vib}) of the $\nu = 3$ to 9 vibrational levels of H_2^+ to be analyzed. The reaction cross section values for D_2^+ at these seven E_{vib} values were determined from the corresponding $\sigma(\nu)$ versus ν curves through interpolation. The results obtained, expressed in terms of the $\sigma(\text{Ne} + \text{D}_2^+)/\sigma(\text{Ne} + \text{H}_2^+)$ ratio, are presented in Figure 4.

Overall, the $\sigma(\text{Ne} + \text{D}_2^+)/\sigma(\text{Ne} + \text{H}_2^+)$ ratio versus E_{vib} tends to decrease with vibrational excitation, although the dependence is not monotonic. In fact, for all E_{col} , there is a minimum and a maximum in the evolution of this ratio from $E_{\text{vib,lowest}} = 0.9062$ eV (vibrational energy of H_2^+ ($\nu = 3, j = 0$)) to $E_{\text{vib,highest}} = 2.0514$ eV (vibrational energy of H_2^+ ($\nu = 9, j = 0$)).

With the exception of what happens at the lowest E_{vib} analyzed, $\sigma(\text{Ne} + \text{D}_2^+)$ is smaller, although not far from $\sigma(\text{Ne} + \text{H}_2^+)$; the smallest values of $\sigma(\text{Ne} + \text{D}_2^+)/\sigma(\text{Ne} + \text{H}_2^+)$ are reached at $E_{\text{vib,highest}}$. (The ratio values are within the 0.65 to 0.76 interval, depending on E_{col}). This result could be interpreted based on the fact that it is easier for $\text{Ne} + \text{H}_2^+$ to achieve a favorable orientation geometry for the reaction to occur than it is for $\text{Ne} + \text{D}_2^+$ because of the smaller inertia momentum of the former molecular ion (see, for example, ref 26).

To try to better understand the intermolecular isotope effect, we can try to think in classical terms and take into account the fact that the maximum impact parameter (b_{max}) has a simple relationship with the maximum J value (J_{max}). ($b_{\text{max}} = J_{\text{max}} \hbar / (2\mu E_{\text{col}})^{1/2}$ for $j = 0$, where all symbols have the usual meaning.) From the data of Table 2, we can obtain the J_{max} values of the two reactions for the E_{vib} interval analyzed. The J_{max} ($\text{Ne} + \text{H}_2^+$) values are clearly below the J_{max} ($\text{Ne} + \text{D}_2^+$) values. From these J_{max} values, one can see that the b_{max} values of both reactions are quite close to each other, and this suggests that the origin of the isotope effect mainly comes from the reaction

probabilities because it is well known that $\sigma(\text{QCT}) = \pi b_{\text{max}}^2 \langle P \rangle$, where $\langle P \rangle$ is the average reaction probability.

IV. Summary and Conclusions

The $\text{Ne} + \text{H}_2^+$ ($\nu = 0-9, j = 0$) and $\text{Ne} + \text{D}_2^+$ ($\nu = 0-12, j = 0$) proton transfer reactions, which are of interest in plasma physics and could be considered to be benchmark systems, were studied at thermal collision energies ($E_{\text{col}} = 0.010$ to 0.14 eV). To do this, the best analytical PES available for the NeH_2^+ system and the CS-RWP quantum dynamics method were employed. To the best of our knowledge, this is the first high-level quantum dynamics calculation where the influence of very high vibrational levels of reactants on the dynamics has been considered.

The CS-RWP reaction probabilities and cross sections for $\text{Ne} + \text{H}_2^+$ ($\nu = 0-9, j = 0$) and D_2^+ ($\nu = 0-12, j = 0$) at around room temperature E_{col} present features similar to those reported in our recent CS-RWP study of the $\text{Ne} + \text{H}_2^+$ ($\nu = 0-4, j = 0$) proton transfer reaction at moderate to intermediate E_{col} (~ 0.3 to 1.7 eV) with the presence of many resonances over the whole energy range because of the influence of metastable states on the dynamics. Furthermore, vibrational energy is more effective than relative translational energy for the reaction to take place, as expected for a late barrier system. (Here the barrier corresponds to the reaction endoergicity.) The CS-RWP relative reaction cross sections at thermal collision energy (300 K) for $\text{Ne} + \text{H}_2^+$ ($\nu = 0-9, j = 0$) and $\text{Ne} + \text{D}_2^+$ ($\nu = 0-12, j = 0$) are in good agreement with the measured data.

The results shown here suggest the adequacy of the CS-RWP approach in describing these and related systems at thermal collision energies and from low to high vibrational excitation of the reactant molecules. This method is numerically very efficient and computationally much less demanding than an exact quantum dynamics treatment.

Acknowledgment. This work was supported by the Spanish Ministry of Education and Science (project no. CTQ2005-09334-C02-01) and by the Spanish Ministry of Science and Innovation (project no. CTQ2008-06805-C02-01), and thanks are also given to the “Generalitat de Catalunya” (Autonomous Government of Catalonia, grant no. 2005SGR 00175). J.M.-P. is also grateful to the Spanish Ministry of Education and Science for a predoctoral research grant.

References and Notes

- (1) Dressler, R. A.; Chiu, Y.; Levandier, D. J.; Tang, X. N.; Hou, Y.; Chang, C.; Houchins, C.; Xu, H.; Ng, C. Y. *J. Chem. Phys.* **2006**, *125*, 132306.
- (2) Mayneris, J.; Sierra, J. D.; González, M. *J. Chem. Phys.* **2008**, *128*, 194307.
- (3) Bilotta, R. M.; Farrar, J. M. *J. Chem. Phys.* **1981**, *75*, 1776.
- (4) Klein, F. S.; Friedman, L. *J. Chem. Phys.* **1964**, *41*, 1789.
- (5) van Pijkeren, D.; Boltjes, E.; van Eck, J.; Niehaus, A. *Chem. Phys.* **1984**, *91*, 293.
- (6) Herman, Z.; Koyano, I. *J. Chem. Soc., Faraday Trans.* **1987**, *2*, 127.
- (7) Zhang, T.; Qian, X.-M.; Tang, X. N.; Ng, C. Y.; Chiu, Y.; Levandier, D. J.; Miller, J. S.; Dressler, R. A. *J. Chem. Phys.* **2003**, *119*, 10175.
- (8) Urban, J.; Jaquet, R.; Staemmler, V. *Int. J. Quantum Chem.* **1990**, *38*, 339.
- (9) Pendergast, P.; Heck, J. M.; Hayes, E. F.; Jaquet, R. *J. Chem. Phys.* **1993**, *98*, 4543.
- (10) Kress, J. D.; Walker, R. B.; Hayes, E. F.; Pendergast, P. *J. Chem. Phys.* **1994**, *100*, 2728.
- (11) Gilibert, M.; Blasco, R. M.; González, M.; Giménez, X.; Aguilar, A.; Last, I.; Baer, M. *J. Phys. Chem. A* **1997**, *101*, 6821.
- (12) Gilibert, M.; Giménez, X.; Huarte-Larrañaga, F.; González, M.; Aguilar, A.; Last, I.; Baer, M. *J. Chem. Phys.* **1999**, *110*, 6278.

- (13) Huarte-Larrañaga, F.; Giménez, X.; Lucas, J. M.; Aguilar, A.; Launay, J.-M. *Phys. Chem. Chem. Phys.* **1999**, *1*, 1125.
- (14) Huarte-Larrañaga, F.; Giménez, X.; Lucas, J. M.; Aguilar, A.; Launay, J.-M. *J. Phys. Chem. A* **2000**, *104*, 10227.
- (15) González, M.; Blasco, R. M.; Giménez, X.; Aguilar, A. *Chem. Phys.* **1996**, *209*, 355.
- (16) Gray, S. K.; Balint-Kurti, G. G. *J. Chem. Phys.* **1998**, *108*, 950.
- (17) Balint-Kurti, G. G. *Adv. Chem. Phys.* **2004**, *128*, 249, and references therein. .
- (18) Miquel, I.; González, M.; Sayós, R.; Balint-Kurti, G. G.; Gray, S. K.; Goldfield, E. M. *J. Chem. Phys.* **2003**, *118*, 3111.
- (19) Gamallo, P.; Sayós, R.; González, M.; Petrongolo, C.; Defazio, P. *J. Chem. Phys.* **2006**, *124*, 174303.
- (20) Martínez, R.; Sierra, J. D.; Gray, S. K.; González, M. *J. Chem. Phys.* **2006**, *125*, 164305.
- (21) Martínez, R.; González, M.; Defazio, P.; Petrongolo, C. *J. Chem. Phys.* **2007**, *127*, 104302.
- (22) Mayneris, J.; Martínez, R.; Hernando, J.; Gray, S. K.; González, M. *J. Chem. Phys.* **2008**, *128*, 144302.
- (23) Mayneris, J.; González, M.; Gray, S. K. *Comput. Phys. Commun.* **2008**, *179*, 741, and references therein. .
- (24) Meijer, A. J. H.; Goldfield, E. M.; Gray, S. K.; Balint-Kurti, G. G. *Chem. Phys. Lett.* **1998**, *293*, 270.
- (25) van Pijkeren, D.; van Eck, J.; Niehaus, A. *Chem. Phys. Lett.* **1983**, *96*, 20.
- (26) Martínez, R.; Sierra, J. D.; González, M. *J. Chem. Phys.* **2005**, *123*, 174312.

JP810476W